Lermusiaux, P.F.J., P.J. Haley, Jr., W.G. Leslie, A. Agarwal, O. Logutov and L.J. Burton, 2011. Multiscale Physical and Biological Dynamics in the Philippines Archipelago: Predictions and Processes, Oceanography, Special PhilEx Issue, Submitted.

Multiscale Physical and Biological Dynamics in the Philippines Archipelago: Predictions and Processes

Pierre F.J. Lermusiaux, Patrick J. Haley, Jr., Wayne G. Leslie,
Arpit Agarwal, Oleg Logutov, and Lisa J. Burton

Department of Mechanical Engineering
Massachusetts Institute of Technology

Abstract:
The Philippine Archipelago is remarkable by the complexity of its geometry, with multiple islands and passages, and by its multiscale dynamics, from the large-scale open-ocean and atmospheric forcing to the strong tides and internal waves in narrow straits and at steep shelfbreaks. We utilize our multi-resolution modeling system to predict and study multiscale dynamics in the region, without the use of any synoptic *in situ* data so as to evaluate modeling capabilities when only sparse remotely sensed sea surface height is available for assimilation. We focus on the Feb.-Mar. 2009 period and compare our simulation results to ocean observations. The oceanographic findings include: a presentation of the various biogeochemical features forecast in real-time, a description of the main circulation features, the evolution of flow fields within three major straits, the estimation of transports to and from the Sulu Sea and the corresponding balances, and finally, an investigation of multiscale mechanisms involved in the formation of the deep Sulu Sea water.

1. Introduction

The Philippines Archipelago is a fascinating multiscale ocean region. Its geometry is very complex with multiple straits, islands, steep shelfbreaks and coastal features, leading to partially interconnected seas and basins (see Figure 1). At depths, there are many bathymetric barriers which form a number of semi-enclosed seas. On the east, these multiply-connected domains are dynamically forced by the Western Pacific including the North Equatorial Current, the Kuroshio and the Mindanao Current and their variable dynamics. On the north-northwest, they are forced by the South China Sea and its coastal currents, eddies and jets. The interactions of these forcing at lateral boundaries with the complex geometry drive an abundance of flow features, with varied temporal and spatial scales (Broecker et al., 1986; Metzger and Hurlburt, 1996; Gordon et al., this issue), and multiple feedbacks to the lateral forcing seas. Several surface and sub-surface water masses are advected to the Archipelago, where they interact and every so often mix to form new water properties. Due to the earth's rotation, stratification and complex bathymetry, mesoscale features are created, often with spatially inhomogeneous Rossby radius of deformation. The surface atmospheric fluxes are also multiscale, including interannual variations, monsoon regimes, weather events and topographic wind jets (Pullen at al., this issue; May et al., this issue). Bottom forcing also occur, for example deep waters are known to be affected by geothermal vents (e.g. Gamo et al., 2007). Finally, and as importantly, barotropic tides, often out of phase in the different basins (Logutov, 2008; Sprintall, personal communication), strongly affect flows, especially in shallower regions and straits. Due to the variable stratification, rotation and steep topographies, they drive a wealth of internal tides, waves and solitons, some of which are known to be among the strongest in the world (e.g. Apel et al., 1985). The purpose of the present study is to describe some of these regional ocean features as estimated by a multi-resolution tidally-

Report Documentation Page

Form Approved
OMB No. 0704-0188

1. REPORT DATE	2. REPORT TYPE	3. DATES COVERED
2010		**00-00-2010 to 00-00-2010**

4. TITLE AND SUBTITLE	5a. CONTRACT NUMBER
MultiscalePhysical and Biological Dynamics in the Philippines Archipelago: Predictions and Processes	5b. GRANT NUMBER
	5c. PROGRAM ELEMENT NUMBER
6. AUTHOR(S)	5d. PROJECT NUMBER
	5e. TASK NUMBER
	5f. WORK UNIT NUMBER
7. PERFORMING ORGANIZATION NAME(S) AND ADDRESS(ES) **Massachusetts Institute of Technology,Department of Mechancial Engineering,Cambridge,MA,02139**	8. PERFORMING ORGANIZATION REPORT NUMBER
9. SPONSORING/MONITORING AGENCY NAME(S) AND ADDRESS(ES)	10. SPONSOR/MONITOR'S ACRONYM(S)
	11. SPONSOR/MONITOR'S REPORT NUMBER(S)

12. DISTRIBUTION/AVAILABILITY STATEMENT
Approved for public release; distribution unlimited

13. SUPPLEMENTARY NOTES

14. ABSTRACT

The Philippine Archipelago is remarkable by the complexity of its geometry with multiple islands and passages and by its multiscale dynamics from the large-?‐scale open-?‐ocean and atmospheric forcing to the strong tides and internal waves in narrow straits and at steep shelfbreaks. We utilize our multi-?‐resolution modeling system to predict and study multiscale dynamics in the region without the use of any synoptic in situ data so as to evaluate modeling capabilities when only sparse remotely sensed sea surface height is available for assimilation. We focus on the Feb.-?&#8208 Mar. 2009 period and compare our simulation results to ocean observations. The oceanographic findings include a presentation of the various biogeochemical features forecast in real-?‐time a description of the main circulation features the evolution of flow fields within three major straits the estimation of transports to and from the Sulu Sea and the corresponding balances and finally an investigation of multiscale mechanisms involved in the formation of the deep Sulu Sea water.

15. SUBJECT TERMS

16. SECURITY CLASSIFICATION OF:			17. LIMITATION OF ABSTRACT	18. NUMBER OF PAGES	19a. NAME OF RESPONSIBLE PERSON
a. REPORT **unclassified**	b. ABSTRACT **unclassified**	c. THIS PAGE **unclassified**	**Same as Report (SAR)**	**28**	

driven ocean model for the February and March 2009 period, without any *in situ* data assimilation. Our ocean science focus is on biogeochemical fields and forecasts, transport balances for the Sulu Sea and flow fields in the corresponding straits, and finally formation mechanisms for the deep Sulu Sea water.

The goals of the Philippines Straits Dynamics Experiment (PhilEx) (Gordon, 2009; Gordon et al., this issue; Lermusiaux et al., 2009) were to enhance our understanding of physical and biogeochemical processes and features arising in and around straits, and to improve our capability to predict the spatial and temporal variability of these regions. A specific objective of the modeling research was to evaluate the capability of tuned modeling systems to estimate the circulation features and processes using only historical data sets for initialization and only remotely sensed data for assimilation, for example, satellite sea surface temperature (SST), sea surface height (SSH) and sea surface color (SSC). The applied motivation of this approach is to simulate the very frequent operational situation where no synoptic *in situ* data can be collected and remotely sensed data are the only synoptic information. The scientific motivation is to evaluate the intrinsic capabilities of tuned models, but without assimilation of *in situ* data, and to determine if some dynamics can be simulated without such synoptic *in situ* data.

For our PhilEx simulations, we employ the MIT Multidisciplinary Simulation, Estimation, and Assimilation System (MSEAS Group, 2010). It includes a free surface hydrostatic primitive-equation physical ocean model developed for multiscale dynamics, resolving very shallow regions with strong tides, steep bathymetries and the deep ocean. The system is capable of multi-resolution simulations over complex geometries with implicit schemes for telescoping nesting (Haley and Lermusiaux, 2010) and has an option for stochastic sub-grid-scale representations (Lermusiaux, 2006). The physical model is coupled to multiple biological models (Besiktepe et al., 2003; Tian et al., 2004) and acoustic models (Lam et al., 2009; Lermusiaux et al., 2010). The ocean physics is forced with high-resolution barotropic tides, estimated using nested coastal inversions (Logutov and Lermusiaux, 2008). Due to the complex multi-connected sea domains, all ocean fields are initialized with new objective mapping schemes developed specifically for PhilEx, using fast marching methods (Agarwal, 2009; Agarwal and Lermusiaux, 2010). Sea surface temperature is also used in the initial conditions. There is no *in situ* data assimilation (Lermusiaux, 1999, 2002, 2007; Lermusiaux et al., 2000); the only synoptic data utilized are the sparse satellite sea surface height observations, providing weak corrections every three to five days.

During the two-month long Intensive Observation Period-09 (IOP09), the MSEAS system was employed in real-time, issuing daily physical-biological forecasts. Dynamical descriptions and adaptive sampling guidance were also provided every 3 to 4 days (Lermusiaux et al., 2009). Fields were compared to data sets from ships and gliders when available.

The present work is partly inspired by our experience in coastal regions with complex geometries (Haley and Lermusiaux, 2010), especially with steep shelfbreaks and straits such as the Sicily Strait (Lermusiaux, 1999; Lermusiaux and Robinson, 2001), Massachusetts Bay and Stellwagen Bank (Besiktepe et al., 2003), Middle Atlantic Bight shelfbreak (Lermusiaux, 1999), Monterey Bay shelfbreak (Haley et al., 2009) and Taiwan region shelfbreak (Lermusiaux et al., 2010). However, in addition to being at least an order of magnitude more complex, in a large part due to the very

intricate geometry and multiscale flows, a major difference of the present PhilEx-O9 simulations with these earlier studies is that very little was known about the dynamics in the region prior the three PhilEx expeditions (Gordon et al., this issue). For example, it is interesting to note that for the month of February, there is not one single Conductivity-Temperature-Depth (CTD) profile recorded for the Sulu Sea in the NODC World Ocean Atlas 2005 (WOA05, Locarnini et al., 2006, Antonov et al., 2006), although this database goes back for more than the past 100 years.

In what follows, we first outline our multi-resolution simulation approach and its parameters. We then present selected real-time multiscale forecasting results, focusing on its most novel components: real-time biogeochemical ocean predictions with region-specific biological state initializations and multi-resolution tidal predictions. We then describe a subset of our re-analysis modeling results with comparisons to ocean observations. We report the major circulation features estimated and discuss our estimates of transports to and from the Sulu Sea as well as the flow fields in the corresponding straits. Finally, we examine the multiscale formation mechanisms for the deep Sulu Sea water.

2. Simulation Methodologies and Parameters

***Multi-resolution Simulations*:** The MSEAS ocean modeling system (Haley and Lermusiaux, 2010) solves the oceanic primitive-equations (PEs) with a nonlinear free surface and tidal forcing. It employs a conservative structured finite-volume grid with time-dependent discretizations and 2-way nesting for multi-resolution, telescoping domains. The resulting schemes are suitable for realistic data-driven multiscale simulations over deep seas to very shallow coastal regions with strong tidal forcing. We employ second order temporal and spatial discretizations that account for the time variations in the finite volumes and nonlinear free surface, and include spherical coordinates and generalized vertical grids. Along with the PE model are modules for data assimilation, atmospheric and tidal forcing, parameterizations for river input and sub-gridscale processes, feature models (Gangopadhyay et al., 2003), and a suite of coupled biological (NPZ) models. In the present PhilEx-09 multi-resolution simulations, we utilize the two-way nesting scheme fully implicit in space and time, i.e. such that within each time-step, updated field values are exchanged across scales and nested domains as soon as they become available. This can be contrasted with explicit nesting schemes which exchange coarse and fine domain fields only at the start of a discrete time integration or time-step. With this nesting scheme, we also use different parameterizations for the sub-gridscale physics in each of the nested domains. Numerical and theoretical analysis of these schemes can be found in Haley and Lermusiaux (2010).

***Modeling Domains and Bathymetry*:** For the PhilEx region**,** we employ spherical coordinates and six 2-way nested domains in telescoping set-ups (Figure 1), ranging from a 3267x3429 km regional domain at 27 km resolution (not depicted) down to a pair of roughly 170x220 km strait domains with high (1km) resolution. The simulations shown in what follows are for the Feb-Mar 2009 period, focusing on the 1656x1503 km Philippine archipelago domain (9 km resolution), the 552x519 km Mindoro Strait domain (3 km resolution) and the 895x303 km Mindanao domain (3 km resolution). All domains have 70 vertical levels arranged in a double-sigma configuration, optimized for the local steep bathymetry and depths of thermoclines/haloclines.

Due to the complexity of the region, we found that the V12.1 (2009) of the Smith and Sandwell (1997) topography was not always very accurate, at times too shallow compared to the depth of ocean water measurements or very different from bathymetric ship data. Since topography is a key variable in the region, in the present simulations, we therefore updated the V12.1 (2009) topography with bathymetry extracted from hydrographic profile data (C. Lee, personal communication) and ship bathymetry and hydrographic data (Gordon and Tessler, personal communication). Specifically, we replaced the Smith and Sandwell data if the hydrographic data were deeper or if ship bathymetry data was available, solving a local diffusion equation (MSEAS Group, 2010) to merge the data sources and ensure bathymetric continuity.

***Initial and Boundary Conditions*:** Simulations were initialized using NODC World Ocean Atlas 2005 (WOA05) climatological profiles (Locarnini et al., 2006, Antonov et al., 2006). WOA05 profiles for the month of February were used for the 0-1500m depth range and Winter profiles from 1500m to the bottom. The profiles were gridded using a new objective analysis scheme (Agarwal and Lermusiaux, 2010) which computes the length of shortest sea paths among model and data points using the Fast Marching Method (FMM) and then uses these distances in the covariance models. Since the NODC database does not contain any CTD observations in February (Sect. 1), the WOA05 climatology estimates the salinity of the Sulu Sea in February as an unrealistic mixture of surrounding water masses. We had to correct for this, using our new objective analysis and initialization schemes. Specifically, since of our goal is to only utilize historical data, we initialized our re-analysis for February in the Sulu Sea using historical CTD data for the month of March. This ensures that Sulu Sea water masses are in the Sulu Sea. The same occurs for the Bohol Sea and we had to proceed similarly.

Also used for the initial conditions are sea surface height anomaly data from the University of Colorado (Leben et al., 2002) and sea surface temperature fields from the GODAE High Resolution Sea Surface Temperature Pilot Project (GHRSST-PP), provided by the UK National Centre for Ocean Forecasting through the Operational Sea Surface Temperature and Sea Ice Analysis (OSTIA) program. The SSH data were converted to surface pressure by multiplication with ρg . From this pressure field, a surface velocity anomaly was constructed from weak geostrophic constraint. The magnitudes of these anomalies were limited to 40 cm/s by a hyperbolic tangent scaling factor applied to speeds greater than 20 cm/s. The resultant velocities were extended in the vertical using a Gaussian covariance with a 500 m decay scale. The SSH and SSH-derived velocity anomaly fields were then merged as weak constraints with the surface elevation and velocity derived from the gridded WOA05 profiles. All of simulations presented next are initialized on February 2, 2009.

For open boundary conditions (OBC), the transports from HYCOM (Bleck, 2002), obtained from NRL-Stennis (Metzger, Hurlburt et al., pers. com.) were merged with the transports derived from the gridded profiles and satellite SSH anomalies. For surface boundary conditions, in real-time (see Sect. 3), we employed COAMPS fluxes for wind stress (0.2 degree resolution, Hodur, 1997) and NOGAPS fluxes for net heat flux and evaporation-minus-precipitation (1.0 degree resolution, Rosmond, 1992). Subsequently, extensive evaluations of atmospheric forcing surface fluxes were completed and for the re-analysis results (Sect. 4), COAMPS archive fluxes (27km/9km resolution, Hodur, 1997) for wind stress, net heat flux and evaporation-minus-precipitation are employed.

For batrotopic tidal forcing, we utilize our multi-resolution tidal elevation and velocity estimates (Logutov, 2008; Logutov and Lermusiaux, 2008), which are derived by generalized inversion from global tidal estimates (Egbert et al., 1994; Egbert and Erofeeva, 2002). Our tidal fields are added as time-dependent external forcing at the OBCs of our free-surface simulations. The barotropic tidal elevations and velocities are also added to the initial subtidal conditions.

***Data for Assimilation and Model Evaluation*:** SSH anomalies are the only synoptic data assimilated when available, about every 4 days to a week. No *in situ* synoptic data are used since one of the PhilEx goals is to evaluate if only assimilating remotely sensed data in tuned models can capture some dynamics. Our total dependency on remotely sensed satellite data to initialize and maintain the synoptic features is one of the novel aspects of the present study.

Measurement data available for evaluations of model estimates and for data-model comparisons include: 125 CTD stations, underway temperature and Acoustic Doppler Current Profiler (ADCP) velocities from the R/V Melville (Gordon, this issue; Tessler et al., 2010); ADCP data from PhilEx moorings (Sprintall, personal communication); drifters (Ohlmann, this issue); profiles from the Global Temperature and Salinity Profile Project (GTSPP); and profiles from the EN3 data set of the UK Meteorological Office, Hadley Centre (Ingleby and Huddleston, 2007).

In total, for the derivation of new methods and codes for generic Archipelago regions and for physical, biogeochemical and numerical parameter tuning and real-time forecasting, more than 3,000 simulations were so far run in this region, for the three expedition periods of 2007, 2008 and 2009. Only a subset of the real-time results and of the re-analysis studies is provided next.

3. Selected Real-time Prediction Results

Due to the complexity of the Archipelago, very significant model improvements were completed prior, during and after the three real-time experiments. Of course, various model parameters (bottom friction, mixing, etc.) were tuned, but more importantly, new methods were developed and software built for complex Archipelagos with topographic barriers and multiply-connected domains. These include new schemes for: i) objective mapping using Fast Marching Methods (Agarwal, 2009; Agarwal and Lermusiaux, 2010); ii) optimizing the many inter-island transports in initializations from geostrophic shear (Agarwal et al., 2010); iii) region-dependent biological initialization; iv) multiscale fully implicit two-way nesting (Haley and Lermusiaux, 2010); and iv) generalized inversion for high-resolution barotropic tidal fields (Logutov and Lermusiaux, 2008). Without these schemes, we could not model the region. During the real-time 2009 exercise (Lermusiaux et al., 2009), forecasts of physical and biological fields were generated at three to four day intervals; remotely sensed products (SST, SSC, SSH) were acquired and utilized; and descriptive dynamics summaries and adaptive sampling guidance were disseminated. Re-analyses were also completed in real-time, for both the physics and the biology, at various resolutions in the different domains. Only SSH data were assimilated every 4 days to a week (see Sect. 2).

***Coupled Physics-Biology IOP09 Real-time Predictions*:** The Dusenberry-Lermusiaux biological model (Besiktepe et al., 2003) was used. The six state variables were initialized using a new region-dependent procedure, reflecting the many topographic barriers of the Archipelago. First, a

synoptic chlorophyll 3D field was created from satellite Sea Surface Color (SSC) data (Arnone, personal communication) and region-dependent generic profiles. Satellite data were combined over a two weeks period (24 Jan - 07 Feb, 2009) to provide sufficient initialization coverage. The Archipelago domain was divided into four regions that are distinct biologically (South China Sea, Shallow Interior Seas, Sulu Sea and Pacific-Sulawesi Sea). Generic parametric chlorophyll profiles were created for each region, based on experimental data from Cordero, et al. (2007). Final initial profiles were then created by scaling the parameters of the generic profiles at each location such that their integration over the euphotic zone would match the SSC data. The initial nitrate and ammonium fields were then estimated using WOA climatology and our new objective mapping schemes (Agarwal and Lermusiaux, 2010). The remaining phytoplankton, zooplankton and detritus initial fields were then dynamically computed using the biogeochemical reaction terms of our equations in a weak constraint form, with parameters estimated from the literature. Specifically, we integrate the reaction terms with a fixed-point iteration scheme (Chapra and Canale, 2009), leading to fields in a quasi-dynamical equilibrium which depends on the parameters of the equations. Hence, the choice of parameters and of initial conditions is coupled. To evaluate the skill of our real-time biological forecasts, modeled chlorophyll fields were integrated into sea surface chlorophyll and averaged over one week, so as to allow comparisons with weekly SSC composites (Figure 2). The forecast field patterns match the SSC data relatively well, with mean differences on the order of 0.1 mg/m^3.

Specific variability patterns to note during February 2009 are the strong and horizontally extended biological activity in the Sibuyan Sea, in response to the NE Monsoon wind mixing, and in the shallow Cuyo Island West passage, in response to topography-driven sub-surface upwelling of deeper nutrient-rich SSC waters rising on the shelf west of the Mindoro Strait. The model forecasts also captured the blooms in the shallower shelf of the western Sulu Sea, in part driven by inflows through the Balabac Strait (see Sect. 4.1) of nutrient rich waters also from the deeper SSC. Vertical sections (not shown) indicate that part of these shelf blooms are also sustained by internal wave mixing and by the turbulent mesoscale gyres and eddies of the Sulu Sea (Figure 2) interacting with the shallow shelf. Biological blooms driven by internal wave and water mass mixing also occur on both sides of the Sulu Archipelago (south of the Sulu Sea from Borneo to Mindanao), as well as on the northern side of Palawan (see the Chl evolution in both the model and SSC fields, noting that the model forecasts under-estimate the amplitudes of Sulu Archipelago blooms). However and interestingly, south of the middle Palawan and Honda Bay, Chl is forecast and observed to be depleted. A lesser but still visible low Chl pool is also estimated on top the Iligan Bay Eddy, a property previously observed (Cabrera et al., this issue). Note however the coastal upwelling-driven bloom just southwest of the Dipolog, along the Zamboanga Peninsula (Villanoy, this issue). A final highlight of these forecasts is a frequently observed feature in NE monsoon conditions (May et al., this issue; Dolar et al., 2006), the wind-jet driven upwelling off Verde Island Passage north of Mindoro and the corresponding biological bloom being advected offshore into “mushroom” patterns of eddies (Rypina et al., 2010). Our estimates indicate that this bloom and its advection pattern develop in two weeks (Fig. 2). Of course, these physical-biological forecasts were only a first attempt, albeit promising, to predict biogeochemical features in a very complex multi-region-equilibrium Archipelago, and this without any *in situ* data assimilation. Due to couplings, detailed biological dynamics studies would require further improvements in both the physics and the biology, and are beyond the scope of this work.

Inverse High-Resolution Barotropic Tidal Modeling: Tidal forecasts and descriptions were provided to support the observational and modeling work in real-time. The data from ADCP moorings (Sprintall, personal communication) were utilized to tune the tidal model and obtain the inverse estimates of the tidal OBCs, used to force our ocean model. The largest constituents are M2, S2, K1 and 01, leading to both diurnal and semi-diurnal components and interactions.

Tides were found to dominate the dynamics in the Surigao and San Bernardino Straits, with model and observed velocities up to 150 cm/s. The spatial structures of the flow fields through these two straits and shallower seas to the west such as the Sibuyan and Visayan Seas are highly spatially inhomogeneous (Figure 3) which makes the role of models in predicting the flow fields and de-tiding the measured currents indispensable. Our high-resolution inverse techniques (Logutov, 2008) also proved necessary to capture the often abrupt changes of phases of barotropic tidal flow fields through the straits, leading to complex mixing patterns and variability in time within the straits proper. Considering the straits reaching the Sulu Sea, the Balabac Strait to the west and Sibutu Strait to the southwest are also tidally very active, with the Sibutu region known to be a generation site of strong solitons (Apel et al., 1985). To the northeast of the Sibutu but still within the Sulu Archipelago, there are several other shallower straits such as the Basilan Strait and Tapiantana Channel, where tidal effects are also significant. The roles of the Sulu Archipelago Straits and shelfbreaks in the formation of deep Sulu Sea water are discussed in Sect 4.3.

4. Re-Analyses and Selected Physical Dynamics Results

4.1 Circulation Features

Model estimates of the ocean currents and salinity fields averaged over a selected set of depth ranges and over time during 18-25 February, 2009 and during 18-25 March, 2009 are provided on Figure 4. In the following, Figure 5, we provide a complementary comparison of the data collected from the R/V Melville during 28 February – 20 March, 2009 (see Gordon, this issue) with our model estimates at the data times and locations.

From the Pacific Ocean, the North Equatorial Current impinges upon the Philippine archipelago, splitting into two boundary currents (around 14N, Qu and Lukas 2003): the equatorward Mindanao current and the creation of the northward Kuroshio (Fig. 4a). Instead of a laminar stagnation point flow, the separation zone is estimated as a wedge-shaped eddy field separating and joining the two currents. A portion of the Mindanao current flows along the island of Mindanao into the eastern Sulawesi Sea, advecting in the saline Pacific waters between 100-200m (Fig. 4b). North of the Philippines, Pacific waters can enter the South China Sea through the Luzon strait (outside of our Archipelago modeling domain). The Mindoro Strait system (Fig. 4c-e) provides a connection for the South China Sea to the Sulu Sea (through the Panay Sill) and to the Sibuyan Sea (through the Tablas Strait). Near the surface, the flow in the Mindoro/Panay Straits starts out southward on average in February (Fig. 4c) in response to the NE monsoon (May et al., this issue), but swings around to a northward average for last part of February and March (Fig. 4e), consistent with the March 2009 observations of Gordon et al. (this issue) and shown on Fig. 5c. At depth, the flow through this strait is predominantly southward (Fig. 4d), weaker at mid-

depth and much stronger near the bottom (Tessler et al., 2010). At the mouth of the Panay Sill, in the Sulu Sea, the cyclonic surface Panay eddy is present for mid-to-late February (Fig. 4c) before being mostly absorbed into northward surface flow (Fig. 4e). For most of the Feb/Mar 2009 period, the flow in the Tablas strait is weak and variable (into and out of the Sibuyan Sea at different periods, Fig. 4e). The South China Sea has two additional connections to the Philippines Archipelago. The first is through the Balabac Strait. In February/March of 2009, the mean flow through Balabac is eastward into the Sulu Sea (Fig. 4a). The second is through the Verde Island passage directly into the Sibuyan Sea. In our simulations, the weekly mean flow there is variable, changing direction and overall magnitude depending on which week is averaged (not shown). The Sibuyan Sea also has a direct connection to the Pacific Ocean through the San Bernardino Strait. Although tidally very active, the mean flows through the strait are negligible (Fig. 4c-e). This agrees with the observations of Gordon et al. (2010) who found no CTD or ADCP evidence of San Bernardino water penetrating far into the Sibuyan or Camotes Seas.

Further south, in the Bohol Sea, the time/depth averaged (upper 100m) fields show an inflow from the Pacific through the Surigao Strait into the Bohol Sea, joining up with the Bohol jet along the northern edge of the Bohol Sea (Fig. 4f), as was also measured. This is consistent with Gordon et al. (this issue) and Hurlburt et al. (this issue), see also Fig. 5e. The Bohol jet continues through the Dipolog Strait and into the Sulu Sea where it joins a cyclonic eddy and proceeds northward along Negros Island. In the western Bohol, the southern edge of the Bohol jet merges with the cyclonic Iligan Bay eddy (Fig. 4f). In our simulation, during late February, the Iligan Bay eddy bifurcates at its western edge into the main eddy and a coastal current that follows Iligan Bay proper until it rejoins the main eddy near Sulauan Point. At depth (400-500m), the flow through the Dipolog strait is eastward from the Sulu Sea into the Bohol Sea (Fig. 4g, also Gordon et al., this issue). At intermediate depths, the flow through Dipolog is more variable. The Sulu Sea itself has a fairly complex eddy field with a general cyclonic flow. On average over the 2 months period, the Sulu Sea has a net inflow from the Balabac, Mindoro/Panay and Dipolog straits and net outflow through the Sibutu Strait and the Sulu archipelago (Fig. 4a). Although the Sibutu Strait has a net outflow, it is tidally very active and experiences episodic net inflows from the Sulawesi Sea (especially in the bottom layers). The Sibutu Strait tides generate strong internal tides and internal waves (Apel et al., 1985; Jackson et al., this issue; Girton et al., this issue) but we also find strong internal tides and waves along the southern rim of the Sulu Sea by the western half of the Sulu archipelago steep shelfbreak. Smaller but appreciable internal tides/waves also occur along the western edge of the Sulu Sea from Borneo across the Balabac Strait to Palawan Island. These sites provide a mixing mechanism for the generation of Sulu deep water (Sect. 4.3).

To compare our model estimates to data, we show in Figure 5 the temperature measurements from 125 CTD stations (Fig. 5a) and the ship-underway ADCP velocities averaged from the depths of 23 to 55 m in the Mindoro (Fig. 5c) and Mindanao regions (Fig. 5e). The corresponding model estimates are given in Figs. 5b, d and f, respectively. The evolution of the temperature profile and the main thermocline along the ship tracks (Fig. 5a) is relatively well captured by our simulations (Fig. 5b), except for the atmospheric-driven surface cooling and upwelling at the end of the track in the Mindoro region which is too strong (simulations without atmospheric forcing maintain the surface temperature structure). Also present in the simulations are some faster internal tides and waves effects (a strong one just before profile 80 is almost at the right time), that even though the

model resolution is still too coarse to capture all finer observed scales. The surface velocities simulated in the Mindoro region (Fig. 5d) are all overall in the right directions, showing the northward flow within the Mindoro Strait into the South China Sea, the Panay Eddy and several features of the Sibuyan Sea. However, model currents are there a bit too weak, likely due to the larger-scale forcing by remotely sensed SSH which is often erroneous in shallower regions and due to the lack of fine-scale *in situ* hydrographic features in the initial conditions (no *in situ* data is used). In the Bohol Sea, model estimates (Fig. 5f) are in close agreement with observations, showing all features, with the exception of parts of the return flow of the Iligan Bay eddy which is weaker in the model during that period, even though it is simulated at most other times (Fig. 4f). This is again due to the assimilation of SSH data, which we found erroneous during that period.

4.2 Flows within Straits and Transports to the Sulu Sea

In Figure 6, we compare the time-series of measured and simulated along-strait velocities at the Panay, Mindoro and Dipolog moorings (Sprintall, pers. com.). Our simulated flows through the straits proper are in generally good agreement with the strength, direction and structure of the observed flows; e.g. the bottom intensified flows at Panay and Dipolog. This is a significant result since many factors could lead to large differences, including: (i) no synoptic *in situ* data is used in the simulation, not even in the initial conditions; (ii) the local bathymetry is very tortuous, uncertain and only simulated at 3 km resolution; and iii) the assimilation of SSH every three days to one week does not resolve strait flows. The first common property is that tidal effects are clearly significant. At Panay (Figs a, d), the simulated along-strait bottom flow is negative, to the Sulu, but is a bit underestimated due to the limited bathymetric resolution and lack of synoptic data. The mid-surface flow is weak, tidally-modulated and on average southward to the Sulu but starts to reverse by the second week of March. The surface flow is northward to the South China Sea as observed, except at the start of the simulation likely due to too large COAMPS wind forcing. At Mindoro (Figs. b, e), as observed, the surface and mid-depth flows are weak and southward, progressively reversing with time and depth. The surface flow converts northward to the South China Sea in March while the mid-depth flow becomes a weak northward flow by the second week of March. At the bottom, the flow remains to the south into the Sulu Sea, but is again a bit too weak in the simulations, largely due to the 3km resolution bathymetry. At Dipolog (Figs. c, f), the surface (negative) along-strait flow is correctly to the Sulu Sea within the Bohol jet and the bottom intensified overflow is from the Sulu Sea to the Bohol. At mid-depths, the flow is more variable, with 14 days period events indicating a progressive mid-depth to mid-surface intensification of inflows to the Bohol, superposed onto mid-depth outflows to the Sulu. All of these simulated properties agree with the synthesis of Gordon et al, this issue.

In Figure 7, we compare the time-averaged values of the above velocity profiles, providing now both the along-strait and across-strait time-averaged velocities. The mean profiles confirm all of the along-strait findings shown on Fig. 6, this time on time-averages. What is perhaps more surprising is that even the across-strait mean flows are relatively well captured, that even though the nested-domain resolution is still a bit too coarse for these smaller scales processes in part controlled by each strait's width, which can very short at depth. It is only for the deep Dipolog that the shape of the across-strait flow is off. This is due to the sharp meanders of the real Dipolog at depth which are not represented in the 3km resolution bathymetry.

The above comparisons were at single mooring positions located at the expected sills of each strait so as to sample the deepest overflows. To extend these results, we now examine the overall water transports across sea segments between islands, focusing on the Sulu Sea during PhilEx-09. To accurately estimate these transports into and out of the Sulu Sea, we employ an algorithm consistent with the conservation of mass imposed by our nonlinear free surface model (see eqn. 65 in Haley and Lermusiaux, 2010). Specifically, the transport along a line segment is the integral of the terms in the divergence operator along model grid edges that best approximate the given line segment. To find that set of grid edges, we employ the Bresenham (1965) line algorithm. The resulting transports are plotted as functions of time in Figs. 8b-f (positive outward), for each of the five open-sea segments surrounding the Sulu Sea (Fig. 8a). Through the segment spanning the Sulu Archipelago (Fig. 8b), we find a time-average mean 3.47 Sv outflow to the Sulawesi Sea (half of which flows through the Sibutu Strait), with a large tidal signal that gives rise to a standard deviation in time of 7.5 Sv. The interplay of diurnal and semi diurnal tides produces a beat pattern envelope on the tidal signal leading to several periods of intense instantaneous inflow across the archipelago from the Sulawesi. The remaining sections, on average, contribute to a mean inflow into the Sulu Sea. The Mindoro strait (Fig. 8c, spanning Palawan to Panay) provides a mean 1.65 Sv inflow with a mostly tidally-driven standard deviation of 2.4 Sv. The mean is consistent with observation of Sprintall (2010) who reports a 1-2 Sv southward averaged transport in Panay Strait during the PhilEx-09 period (the NE-Monsoon driving stronger than normal mid-depth southward flow in this strait). The Balabac Strait (Fig. 8d) provides a mean 1.04 Sv with a mostly tidal 0.7 Sv standard deviation in time. The Diplolog strait (Fig. 8e) provides a mean 0.79 Sv with a 1.4 Sv standard deviation. In the Guimaras Strait (between Panay and Negros, Fig 8f), there is essentially no net flow (8×10^{-4} Sv mean inflow with 0.002 Sv standard deviation). Summing the inflows of these four sections provides a mean 3.48 Sv inflow. The difference between this mean inflow and the above mean outflow is a net 0.01 Sv inflow. This is exactly equal to the free-surface term in our model equations and is equivalent to a mean 3mm rise in the Sulu SSH over a time step of 150sec. Of course, all of these transports and temporal variability are uncertain. Based on the ensemble of simulations that we ran, the mean transport uncertainties are about 50%. These numbers also depend on the open boundary inflows from the Pacific (e.g. Arango et al, this issue).

4.3 Deep Sulu Sea Water

The Sulu Sea is a semi-enclosed basin filled and renewed by waters overflowing the above-mentioned straits and open-sea segments (Sect 4.2). Its deep water has received recent attention in part because of decadal and climate studies (e.g. Quadfasel et al, 1990; Rosenthal et al, 2003; Gamo et al, 2007; Gordon et al, personal communication). Below 1250m, salinity is observed to be slightly stratified from a minimum of 34.45 to the deep salinity reaching 34.744, while the temperature is relatively uniform, suggesting that the deep water is a mixture of water masses. We now examine the multiscale processes likely responsible for this deep water formation.

The two deepest straits leading to the Sulu Sea are the Panay Sill to the northeast (depth of sill around 570m) and Sibutu Strait to the southwest (depth of sill near Pearl Bank around 370m). In Figure 9, we show their location (Fig. 9a) and the corresponding deep transports as a function of time (Figs. 9b and 9d). Studying the Panay Sill first, our results show a net time-average deep

inflow of 0.645 Sv to the Sulu (Fig. 9b), with a 50% uncertainty standard deviation, and a 0.2Sv tidal modulation. The mean transport is about twice as large as that obtained by Tessler et al. (2010), which is within our uncertainties. These authors used the mooring data for the same Feb-Mar 2009 time frame and extended the point profile in space using triangular shapes to obtain a bottom transport. Several reasons can explain the difference. First, slight changes in that shape or in its extension alter the final estimate. Second, the mooring is at the Sill proper and does not sample the whole flow. In fact, the time-averaged velocity section (Fig. 9c) reveals an intensified current to the western side of the Sill. This agrees with a southward density-driven flow along the Mindoro-Panay Strait system and momentum advection in approximate balance with the Coriolis force and bottom stress, with the former deflecting the flow to the right. This finding of western-side intensified flow agrees with hydrographic data (Tessler et al., 2010). Finally, it is worth noting that if we restrict our bottom transport to salinities within 34.43 to 34.46 (not shown), we would divide our transport by more than two. Focusing now on the Sibutu Strait, our simulation shows a deep flow (Fig. 9d) with strong tidal velocities, but a small net time-averaged inflow of 0.032 Sv into the Sulu Sea during Feb-Mar 2009. However, also visible are periods of intense instantaneous deep inflow from the Sulawesi, modulated by spring and neap tides, at approximately twice a month to a month frequency. This is confirmed by the salinity at the strait section (Fig. 9a) spatially-averaged within 20m of the bottom (Fig. 9e); the deep mean salinity at Sibutu is indeed driven by such slower frequencies, increasing to 34.59 in periods of inflow from the Sulawesi.

To confirm that these two straits are the two main sources for the deep salty Sulu water, we first focus on the overflows from deep depths. We show in Fig. 10a the salinity integrated vertically at each model grid point from 200m to 1000m depths, but only if the salinity is within 34.45 to 34.55 (salinities outside that range are not considered), and averaged over Feb. 4 to 11, 2009. The corresponding integrated and averaged horizontal velocity is shown on Fig. 10b. Clearly visible are the Mindanao current advecting higher salinities from the sub-surface Pacific waters to the Sulawesi, which can ultimately reach the Sibutu. Also shown are the smaller but still sufficient salinities of the South China Sea, which flow in the Mindoro-Panay Strait system. Overall, the Panay Sill provides averaged salinities around 34.47 to 34.52 while the Sibutu provides averaged salinities around 34.5 to 34.55, with mixing occurring with each strait. Also shown are upwelling along the steep shelfbreaks in the region. The tidally active Balabac Strait (sill depth around 100m) could thus at times be a source, but our present simulations did not show significant inflow events. Finally, visible in the Sulu Sea just north of Sibutu and the Sulu Archipelago (Fig. 10a) are strong internal tides/waves signals suggesting a mechanism for deep mixing. This is required since the highest mean salinities in the Sulu Sea are below 1000m.

In Figs. 10c-d, we illustrate the mixing and upwelling/downwelling patterns occurring at Sibutu. Considering first pure mixing, within the 100 to 200m layer, two water masses collide and can be tidally mixed at the sills of Sibutu: the sub-surface modified salty Pacific waters advected in from the Sulawesi and the sub-surface waters of the Sulu Sea (less salty at those depths in part due to inflow of more-modified Pacific waters from the South China Sea). Now considering upwelling, we show in Figs. 10c-d that deep waters below 700m can upwell to 200m, mix within the complex Sibutu Strait sills and sub-basins, and finally flow into the Sulu Sea. Our simulations also reveal that these waters can then either downwell and further mix along the steep Sulu bathymetry or advect on the narrow shelves of the Sulu Archipelago. Of course, the vertical velocity patterns

(Fig. 10d) oscillate with tides (of different phases on each side of the strait) and are not permanent. However, the neap and spring cycles lead to periods favorable to mean upwelling from the deep Sulawesi (see Fig. 9e). We find that mixing occurs at the entrance of Sibitu and at the exit of Sibutu within internal waves, but we also discover stronger internal waves all along the steep shelfbreak on the northern side of the Sulu Archipelago (Fig. 10e-f). Several of these waves would develop into deep solitons in the real ocean. We note that the northern Sibutu and Sulu Archipelago shelfbreak waves are not in phase, but that stronger tidal events occur every 14 days or so at both locations. These events lead to vigorous mixing of the high salinity waters (not shown). To illustrate the circulation and mixing in the Sulu Sea, we show the depth of the surfaces of constant potential density anomaly σ_θ=26.15 and σ_θ=26.50 (Figs. 10g and 10i), and the salinity fields on these two surfaces (Figs. 10h and 10j), all estimated on Feb 20 at 19:30Z. The inflow from the Mindoro-Panay Strait system is clearly visible (Fig. 10h). At Sibutu, but even more so along the Sulu Archipelago, several train of internal waves have developed (compare with the first week of Feb. on Fig. 10a). As the saltier waters are mixed down at depth, they form a tongue of higher salinity on which other deeper internal waves can ride, further increasing the mixing. Note that these deeper internal waves travel at an angle from the Sulu Archipelago (e.g. Fig. 10h). The salinity tongue also creates horizontal density gradients which displace the overall cyclonic circulation further offshore, ultimately creating anticyclones on both sides of the tongue (e.g. by the end of Feb, not shown). The depth of σ_θ=26.50 (Fig. 10i) reveals a main driver for this tendency towards cyclonic circulation in the Sulu Sea, the sinking, mixing and advection of heavier salty waters along all of its slopes. The highest salinities on σ_θ=26.50 (Fig. 10j) confirm the advection form the Sibutu. However, the strongest mixing and sinking occurs at the steep shelfbreak in the middle of the Sulu Archipelago: salinity on σ_θ=26.55 (not shown), clearly shows that it is the fastest there, reaching a depth of 1800m in 3 weeks.

5. Conclusions

The Philippine Archipelago region is striking by the complexity of its geometry, with multiple islands and passages, and by the multiscale dynamics, from the North Equatorial Current and open-ocean eddies in the Pacific to the very strong tides in shallow areas and the internal waves at steep shelfbreaks. This complexity required novel schemes, from our multiscale objective-analyses for such regions (Agarwal and Lermusiaux, 2010) to a new time-dependent spatial discretizations and fully-implicit two-way nesting in telescoping domains (Haley and Lermusiaux, 2010). Without these schemes, such multiscale simulations were not possible. In the present study, the modeling focus was on the utilization of tuned models using no *in situ* synoptic data but only infrequent and sparse remotely sensed sea surface height data.

As described in this special issue, not much was known quantitatively about the region prior to the PhilEx program and its three sea campaigns. The simulations presented here focus on the PhilEx-09 period during Feb.-Mar. 2009. The real-time results we illustrated include a description of different biogeochemical features forecast in real-time as well as our multi-resolution tidal predictions for the region. The other ocean science findings presented consist of: a description of the main circulation features estimated in the whole Archipelago region and its many seas; the evolution in time and depth of currents above the deepest point of three major straits and a comparison of these estimates to data; the estimation of transports to and from the Sulu Sea and

the corresponding overall water mass balance; and finally, an investigation of multiscale mechanisms involved in the formation of the deep Sulu Sea water.

Opportunities for future multiscale dynamical and process studies are plentiful. They include: physical and biological-physical dynamics in each strait (e.g. San Bernardino, Surigao, Mindoro, Dipolog, Sibutu, Balabac) and in specific circulation features such as the Iligan Bay Eddy; dynamics of Sulu Sea gyres and their relationships with overflows and mixing; detailed multiscale dynamics involved in the formation of the deep Sulu Sea water; relative contributions of wind-driven vs. density-driven vs. tidally-driven circulations, from the shallow to the deep seas; and, impacts of larger-scale transports at open domain boundaries. An ultimate goal would be to connect our results to basin-scale and climate studies.

Acknowledgments
We are very grateful to A. Gordon, Z. Tessler and L. Pratt for many fruitful discussions on ocean dynamics in the region and for their encouragement. We are also thankful to C. Villanoy, C. Lee and J. Sprintall (supported under ONR grant N00014-06-1-0690) for their ocean data, H. Hurlburt and J. Metzger for large scale boundary conditions, and H. Arango, J. Levin and I. Rypina for useful discussions. We also thank J. Doyle, D. Marble, J. Nachimknin and J. Cook as well as the FNMOC for providing us with atmospheric fluxes. Finally, we are thankful to the Office of Naval Research and Dr. Harper for research support under grants N00014-07-1-0473 (PhilEx), and N00014-07-1-1061 and N00014-08-1-1097 (6.1), to the Massachusetts Institute of Technology.

References

Agarwal, A., 2009. Statistical field estimation and scale estimation for complex coastal regions and archipelagos. Master's thesis, Massachusetts Institute of Technology, Cambridge, MA

Agarwal, A. and P.F.J. Lermusiaux, 2010. Statistical field estimation for complex coastal regions and archipelagos. Ocean Modeling, In preparation.

Antonov, J. I., R. A. Locarnini, T. P. Boyer, A. V. Mishonov, and H. E. Garcia, 2006. World Ocean Atlas 2005, Volume 2: Salinity. S. Levitus, Ed. NOAA Atlas NESDIS 62, U.S. Government Printing Office, Washington, D.C., 182 pp.

Apel, J.R., J.R. Holbrook, J. Tsai, and A.K. Liu, 1985. The Sulu Sea internal Solitons experiment. J. Phys. Oceanogr., 15 (12), 1625-1651.

Arango, H. G., J. C. Levin, E. Curchitser, B. Zhang, A. M. Moore, W. Han, A. L. Gordon, C. Lee, and J. B. Girton. 2011. Development of a Hindcast/Forecast Model for the Philippine Archipelago, this issue.

Besiktepe, S.T., P.F.J. Lermusiaux and A.R. Robinson, 2003. Coupled physical and biochemical data driven simulations of Massachusetts Bay in late summer: real-time and post-cruise data assimilation. Special issue on "The use of data assimilation in coupled hydrodynamic, ecological and bio-geo-chemical models of the oceans", *J. of Marine Systems*, M. Gregoire, P. Brasseur and P.F.J. Lermusiaux (Eds.), 40, 171-212.

Bleck, R., 2002. An oceanic general circulation model framed in hybrid isopycnic-Cartesian coordinates, Ocean Modelling, 37, 55-88.

Bresenham, J.E., 1965. Algorithm for computer control of a digital plotter. IBM Systems Journal, 4(1), 25-30.

Broecker, W., W. Patzert, R Toggweiler, M. Stuiver, 1986. Hydrography, chemistry, and radioisotopes in the Southeast Asian Basins. J. Geophys. Res., 91:14,345-14,354.

Cabrera, O.C, C.L. Villanoy, L. T. David, A. L. Gordon, 2011. Barrier Layer Control of Entrainment and Upwelling in the Bohol Sea, Philippines, this issue.

Chapra, S.C. and R. P. Canale, 2009. Numerical Methods for Engineers. McGraw-Hill Higher Education, Boston, sixth edition, 960pp.

Cordero, K., C.L. Villanoy, L.T. David and K. Silvano, 2007. Estimating integrated phytoplankton biomass in the seas around the Philippines, Proceedings of the 13th Workshop of OMISAR (WOM-13) on Validation and Application of Satellite Data for Marine Resources Conservation, October 5-9, 2004, Bali, Indonesia.

Dolar, M.L., W.L. Perrin, B.L. Taylor, G.L. Kooyman, M.N.R. Alava, 2006. Abundance and distributional ecology of cetaceans in the central, Philippines. Journal of Cetacean Research and Management, 8: 93–111.

Egbert, G. D., A. F. Bennett, and M. G. G. Foreman, 1994. Topex/Poseidon tides estimated using a global inverse model, *J. Geophys. Res., 99,* 24821-52.

Egbert. G. D. and S. Y. Erofeeva, 2002. Efficient Inverse Modeling of Barotropic Ocean Tides, *J. Atmospheric and Oceanic Tech.*, 19, 2, 183-204.

Gamo, T., Y. Kato, H. Hasumoto, H. Kadiuchi, N. Momoshima, N. Takahata, and Y. Sano, 2007. Geochemical implications for the mechanism of deep convection in a semi-closed tropical marginal basin: Sulu Sea. Deep-Sea Res., 54, 4–13, doi:10.1016/j.dsr2.2006.06.004

Gangopadhyay, A., A.R. Robinson, P.J. Haley, W.J. Leslie, C. J. Lozano, James J. Bisagni, and Z. Yu, 2003: Feature Oriented Regional Modeling and Simulation (FORMS) in the Gulf of Maine and Georges Bank, Continental Shelf Research 23(3-4), 317-353.

Gordon, A.L., 2009. Regional Cruise Intensive Observational Period 2009. Tech. rep., Lamont Doherty Earth Observatory, URL http://mseas.mit.edu/Sea exercises/Philex IOP09/RIOP09 LEG2 rept.pdf.

Gordon, A.L., J. Sprintall and A. Ffield, 2011. Regional Oceanography of the Philippine Archipelago, this issue.

Girton, J. B., B. Chinn, and M. H. Alford, 2011. Internal Wave Climates of the Philippine Seas, this issue.

Haley, P.J. Jr., P.F.J. Lermusiaux, A.R. Robinson, W.G. Leslie, O. Logoutov, G. Cossarini, X.S. Liang, P. Moreno, S.R. Ramp, J.D. Doyle, J. Bellingham, F. Chavez and S. Johnston, 2009. Forecasting and reanalysis in the Monterey Bay/California Current region for the Autonomous Ocean Sampling Network-ii experiment. Deep Sea Research II 56(3-5):127–148, doi:10.1016/j.dsr2.2008.08.010

Haley, P.J., Jr. and P.F.J. Lermusiaux, 2010. Multiscale two-way embedding schemes for free-surface primitive-equations in the Multidisciplinary Simulation, Estimation and Assimilation System. Ocean Dynamics. doi:10.1007/s10236-010-0349-4, In press.

Hodur, R.M., 1997. The Naval Research Laboratory's Coupled Ocean/Atmosphere Mesoscale Prediction System (COAMPS), Monthly Weather Review, 125, 7, 1414-1430.

Hurlbert, H., J. Metzger, J. Sprintall, S. N. Riedlinger, R. A. Arnone, T. Shinoda, and X. Xu, 2011. Circulation in the Philippine Archipelago simulated by 1/12° and 1/25° global HYCOM and EAS NCOM, this issue.

Ingleby, B., and M. Huddleston, 2007. Quality control of ocean temperature and salinity profiles - historical and real-time data. *J. Mar. Sys.*, 65, 158-175 10.1016/j.jmarsys.2005.11.019

Jackson, C. and Y. Arvelyna, 2011. High Frequency Nonlinear Internal Waves around the Philippines, this issue.

Jones, B.H., E.S. Boss, M.C. Gregg, C. M. Lee, G. Toro-Farmer and C. Villanoy, 2011. Tidally driven exchange in an Archipelago strait: Biological and optical responses, this issue.

Lam, F.P, P.J. Haley, Jr., J. Janmaat, P.F.J. Lermusiaux, W.G. Leslie, M.W. Schouten, L.A. te Raa, and M. Rixen, 2009. At-sea Real-time Coupled Four-dimensional Oceanographic and Acoustic Forecasts during Battlespace Preparation 2007. Special issue of the *Journal of Marine Systems* on "Coastal processes: Challenges for Monitoring and Prediction", Drs. J.W. Book, Prof. M. Orlic and Michel Rixen (Guest Eds.), 78, S306-S320, doi: 10.1016/j.jmarsys.2009.01.029

Leben, R. R., G. H. Born, and B. R. Engebreth, 2002, Operational altimeter data processing for mesoscale monitoring. *Marine Geodesy*, 25, 3-18.

Locarnini, R. A., A. V. Mishonov, J. I. Antonov, T. P. Boyer, and H. E. Garcia, 2006. World Ocean Atlas 2005, Volume 1: Temperature. S. Levitus, Ed. NOAA Atlas NESDIS 61, U.S. Government Printing Office, Washington, D.C., 182 pp.

Lermusiaux, P.F.J., 1999. Data assimilation via error subspace statistical estimation. Part II: Middle atlantic bight shelfbreak front simulations and ESSE validation. Mon. Wea. Rev. 127(8):1408–1432

Lermusiaux, P.F.J., 2002. On the mapping of multivariate geophysical fields: sensitivity to size, scales and dynamics. Journal of Atmospheric and Oceanic Technology 19(10):1602–1637

Lermusiaux, P.F.J., 2006. Uncertainty estimation and prediction for interdisciplinary ocean dynamics. Journal of Computational Physics 217(1):176–199, special issue of on ”Uncertainty Quantification”. J. Glimm and G. Karniadakis, Eds. 50

Lermusiaux, P.F.J., 2007. Adaptive sampling, adaptive data assimilation and adaptive modeling. Physica D 230:172–196, Special issue on ”Mathematical issues and challenges in data assimilation for geophysical systems: interdisciplinary perspectives”, C. Jones and K. Ide, Eds.

Lermusiaux, P.F.J. and A.R. Robinson, 2001. Features of dominant mesoscale variability, circulation patterns and dynamics in the Strait of Sicily. *Deep Sea Research*, (48), 9, 1953-1997.

Lermusiaux, P.F.J., D.G.M. Anderson and C.J. Lozano, 2000. On the mapping of multivariate geophysical fields: Error and variability subspace estimates. *Q.J.R. Meteorol. Soc.*, 126, 1387-1429

Lermusiaux et al., 2009. Real-time IOP09 Multiscale Field Estimation, Forecasting and Dynamical Descriptions. http://mseas.mit.edu/Sea_exercises/Straits/index.html.

Lermusiaux, P.F.J., J. Xu, C.F. Chen, S. Jan, L.Y. Chiu and Y.-J. Yang, 2010. Coupled Ocean-Acoustic prediction of transmission loss in a continental shelfbreak region: predictive skill, uncertainty quantification and dynamical sensitivities. IEEE Transactions, Journal of Oceanic Engineering. In press, doi: 10.1109/JOE.2010.2068611.

Logutov, O.G., 2008. A multigrid methodology for assimilation of measurements into regional tidal models. *Ocean Dynamics*, 58, 441-460, doi:10.1007/s10236-008-0163-4

Logutov, O.G. and P.F.J. Lermusiaux, 2008. Inverse Barotropic Tidal Estimation for Regional Ocean Applications. *Ocean Modelling*, 25, 17-34. doi:10.1016/j.ocemod.2008.06.004

May, P., J. Doyle, J. Pullen and L. David, 2011. Two-Way Coupled Atmosphere-Ocean Modeling of the PhilEx Intensive Observing Periods, this issue.

Metzger, E. J. and H. E. Hurlburt, 1996. Coupled dynamics of the South China Sea, the Sulu Sea, and the Pacific Ocean. Journal of Geophysical Research, 101(C5): 12331-12352.

MSEAS Group, 2010. The multidisciplinary simulation, estimation, and assimilation systems (http://mseas.mit.edu/, http://mseas.mit.edu/codes). Reports in Ocean Science and Engineering 6, Department of Mechanical Engineering, MIT, Cambridge, Massachusetts

Ohlmann, J. C., 2011. Drifter Observations in the Philippines Archipelago: Regional Circulation and Small-Scale Flows, this issue.

Pullen, J., A. Gordon, J. Sprintall, C. Lee, M. Alford, J. Doyle and P. May, 2011. Winds, Eddies and Flow through Straits, this issue.

Qu, T. and R. Lukas, 2003. The Bifurcation of the North Equatorial Current in the Pacific, J. Phys. Oceanogr., 33, 5–18.

Quadfasel, D., H. Kudrass and A. Frische,1990. Deep-water renewal by turbidity currents in the Sulu Sea. Nature 348:320-322

Rosenthal, Y., D. W. Oppo, et al., 2003. The amplitude and phasing of climate change during the deglaciation in the Sulu Sea, western equatorial Pacific (DOI 10.1029/2002GLO16612). Geophysical Research Letters 30(8): 16.

Rosmond, T.E., 1992. The Design and Testing of the Navy Operational Global Atmospheric Prediction System, Weather and Forecasting, 7, 2, 262-272.

Rypina, I., L. Pratt, J. Pullen, J. Levin and A. Gordon, 2010. Chaotic Advection in an Archipelago. Journal of Physical Oceanography, 40, 1988-2006, DOI: 10.1175/2010JPO4336.1.

Smith, W. H. F., and D. T. Sandwell, 1997. Global seafloor topography from satellite altimetry and ship depth soundings, Science, 277, 1957-1962.

Tessler, Z., A.L. Gordon, L.J. Pratt, J. Sprintall, 2010. Transport and Dynamics of Panay Sill Overflow in the Philippine Seas, Journal of Physical Oceanography, in press.

Tian, R.C., P.F.J. Lermusiaux, J.J. McCarthy and A.R. Robinson, 2004. A generalized prognostic model of marine biogeochemical-ecosystem dynamics: Structure, parameterization and adaptive modeling. Harvard Reports in Physical/Interdisciplinary Ocean Science 67, Harvard University, Cambridge, MA

Villanoy, C., O. Cabrera, A. Yniguez, M. Camoying, A. de Guzman, L. David and P. Flament. 2011. Monsoon-driven coastal upwelling in the Zamboanga Peninsula, Philippines, this issue.

Figures

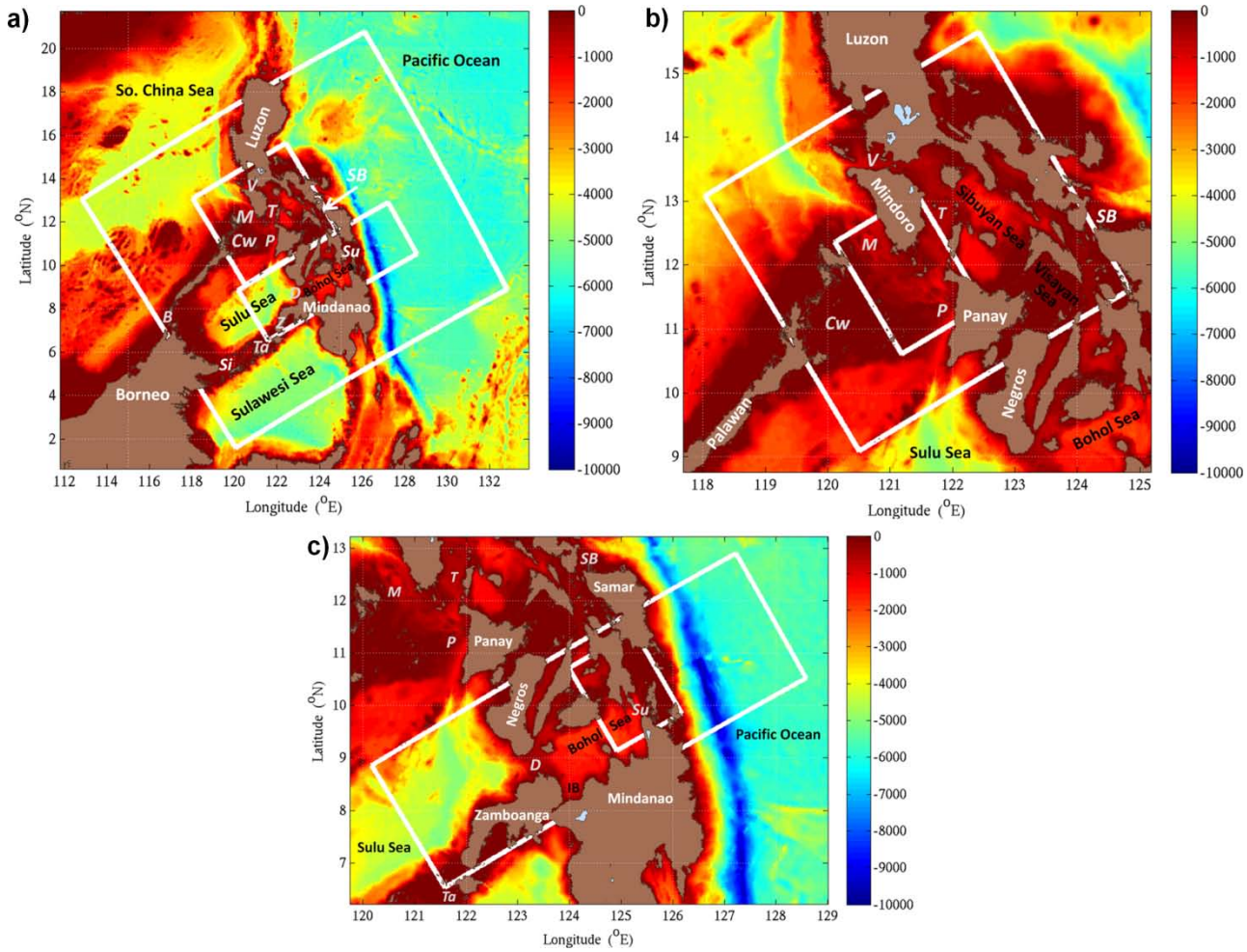

Figure 1 – Spherical-grid domains in a telescoping zoom configuration for our multiscale simulations in the Philippine Archipelago overlaid on our estimate of bathymetry (combining the V12.1 (2009) of the Smith and Sandwell topography with hydrographic and bathymetric ship data). a) Archipelago 9km resolution domain with nested Mindoro (3km) and Mindanao (3km) domains. b) Mindoro Strait 3km and 1km domains. c) Mindanao/Surigao Strait 3km and 1km domains. Straits and local features are identified by one or two-letter abbreviations. Alphabetically these are: B – Balabac Strait, Cw – Cuyo West Passage, D – Dipolog (Mindanao) Strait, IB – Illigan Bay, M – Mindoro Strait, P – Panay Sill, SB – San Bernardino Strait, Si – Sibutu Strait, Su – Surigao Strait, T – Tablas Strait, V – Verde Island Passage, Ta – Tapiantana Strait, Z – Zamboanga Strait

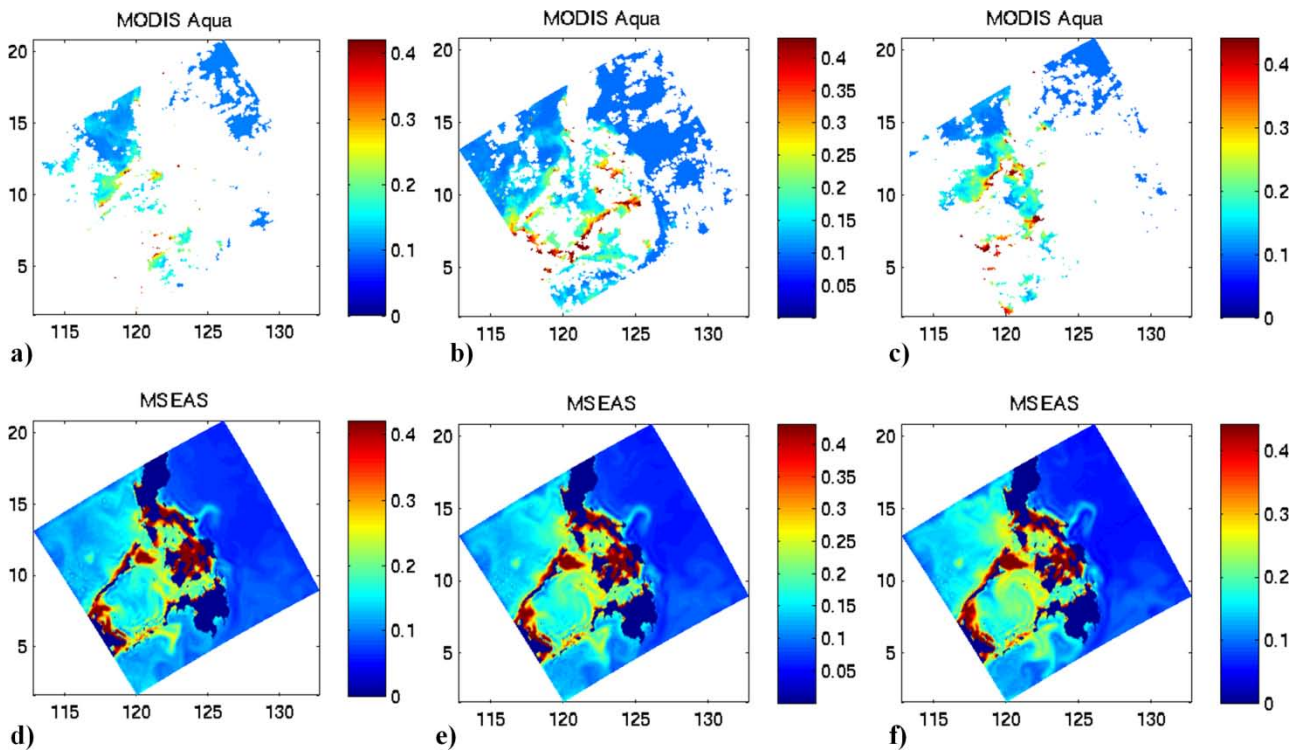

Figure 2 - Comparison of MSEAS chlorophyll near real-time forecasts with composites of satellite SSC imagery. The top panels are the satellite composites, the bottom row are the corresponding MSEAS forecasts. a) and d) 26 Feb. – 4 Mar. 2009; b) and e) 5-11 March 2009; c) and f) 12-18 March 2009. Note that the satellite data is limited due to cloud cover. Modeled chlorophyll forecasts were integrated into sea surface chlorophyll and averaged over one week, so as to allow comparisons with weekly SSC composites. The forecast field patterns match the SSC data relatively well, with mean differences on the order of 0.1 mg/m^3.

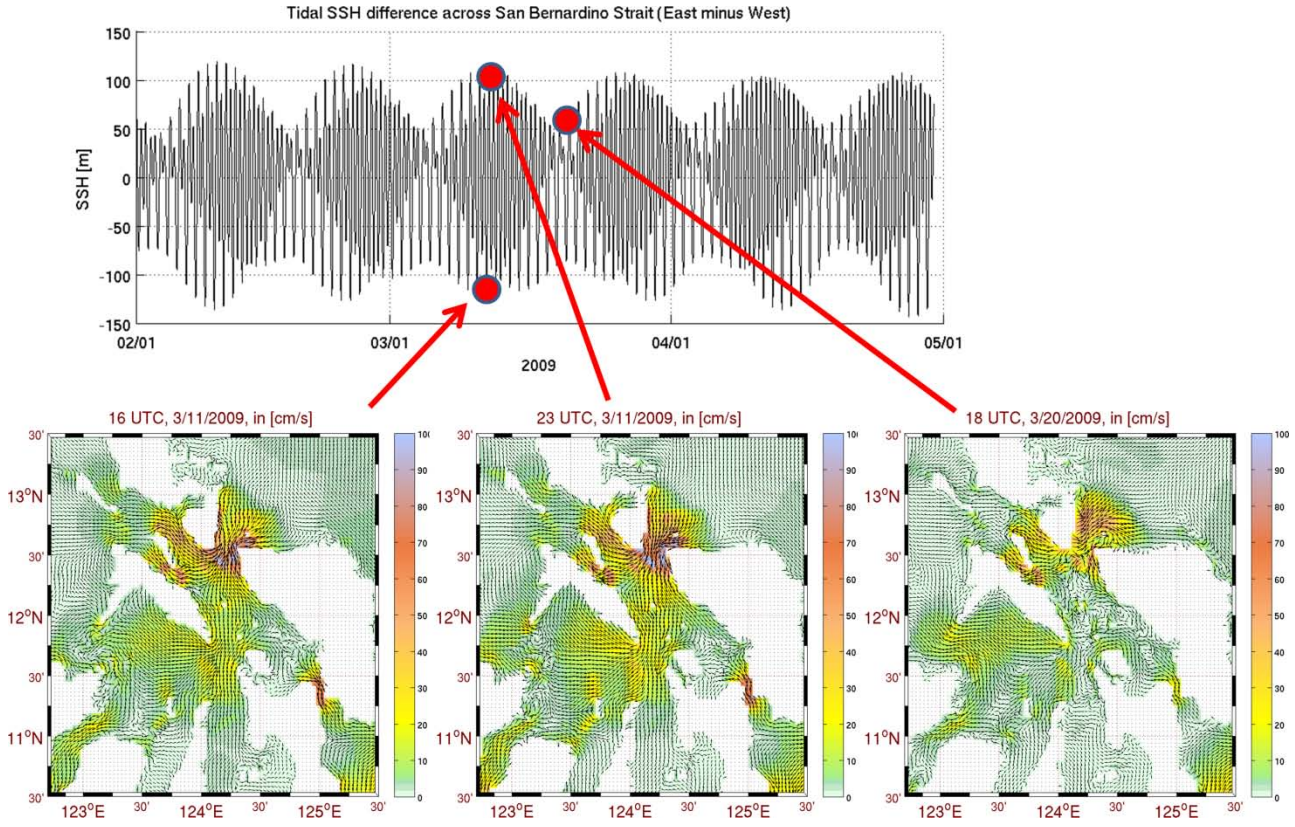

Figure 3. Multi-resolution inverse barotropic tidal model forecasts – illustrating temporal variability and the spatially inhomogeneous nature of tidal flow fields in the San Bernardino and Sibuyan and Visayan Seas region. The top panel illustrates tidal SSH difference across the San Bernardino Strait, the bottom row is the barotropic tidal flow for 1600Z and 2000Z on 11 March 2009, and 1800Z on 20 March 2009, respectively. Our high-resolution inverse techniques using high-resolution bathymetry proved necessary to capture the multiscale tidal flow fields.

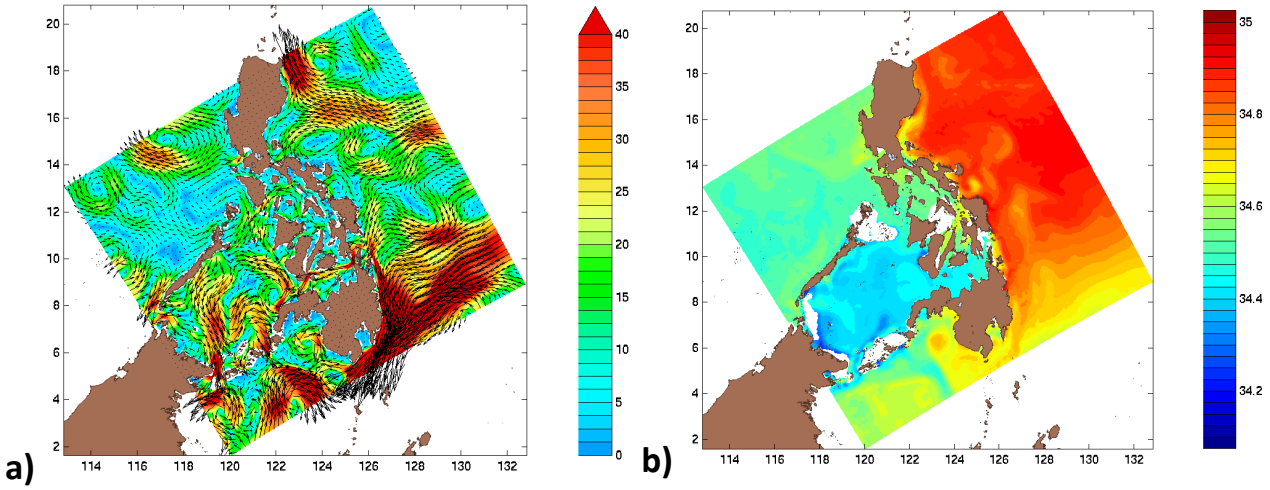
a)
b)
c)
d)
e)

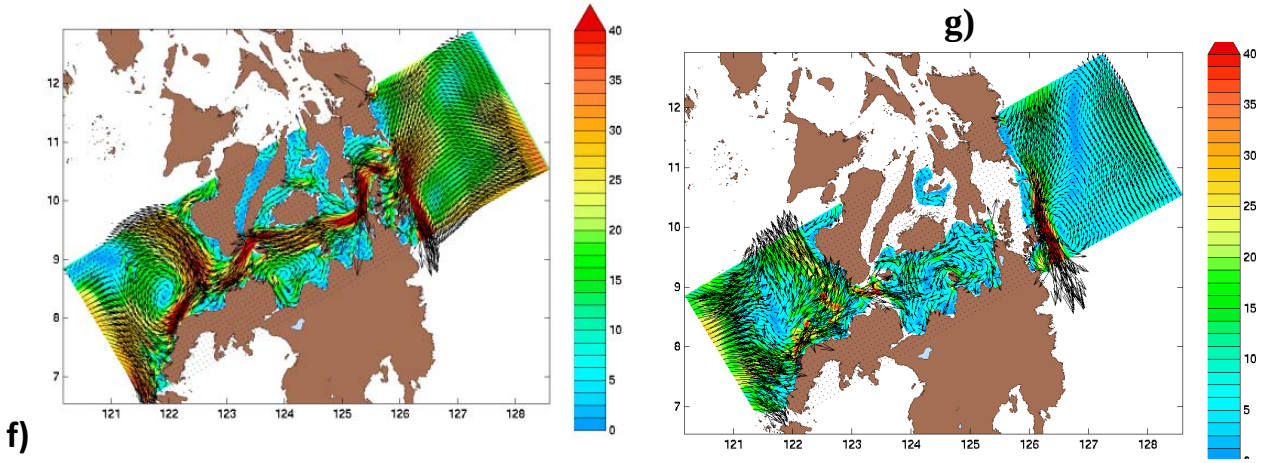

Figure 4 - Time and depth averaged model re-analysis estimates displaying canonical flow features for PhilEx-09. (a) Velocity averaged between 0-100m during 18-25 Feb; (b) Salinity averaged between 100-200m during 18-25 Feb; (c) Velocity in Mindoro domain averaged between 0-50m during 18-25 Feb; (d) Velocity in Mindoro domain averaged between 100-200m during 18-25 Feb; (e) Velocity in Mindoro domain averaged between 0-50 m during 18-25 Mar; (f) Velocity in Mindanao domain averaged between 0-100m during 18-25 Feb; (g) Velocity in Mindanao domain averaged between 400-500m during 18-25 Feb.

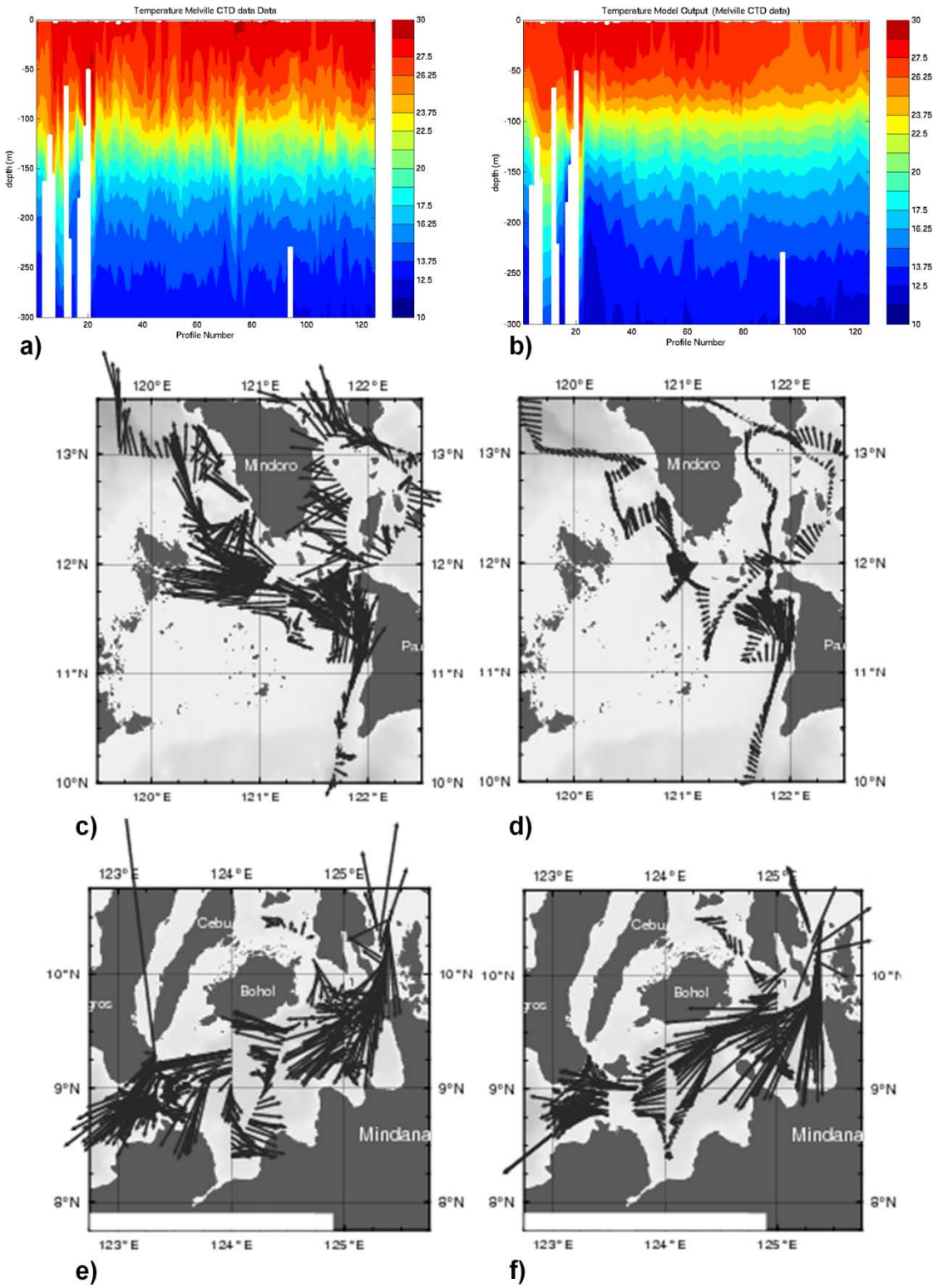

Figure 5 – Comparisons of *in situ* data and model re-analysis results. a) Melville CTD casts and b) model temperature estimates. Melville profiles 1-22 were collected within the San Bernardino region, out to the Pacific and back through shallower seas and island chains towards the Bohol Sea over the period 28 Feb. – 3 Mar., 2009. Profiles 23-40 were collected in 3-5 Mar. 2009 within the Bohol Sea. Profiles 41-63 were collected in the Dipolog (Mindanao) Strait and westward into

the Sulu Sea over the period 5-9 March. The Sulu Sea to the coast of Panay was covered by stations 64-85 from 9-15 March. From 15-17 March the Melville was off Panay, into the Tablas Strait and returned to the Panay Sill region. The Mindoro Strait was sampled from 17-20 March. c) Velocity vectors of underway ADCP data averaged over the depth range 23-55m during 14-20 March. d) Corresponding model velocity vectors. e) as for c), but in the Bohol region during 3-5 March. f) Corresponding model velocity vectors. Model estimates generally reproduce the structures found in the underway ADCP data, but are weaker than observations in the Mindoro region, in part due to the non-use of *in situ* data and to errors in the SSH data and atmospheric forcing.

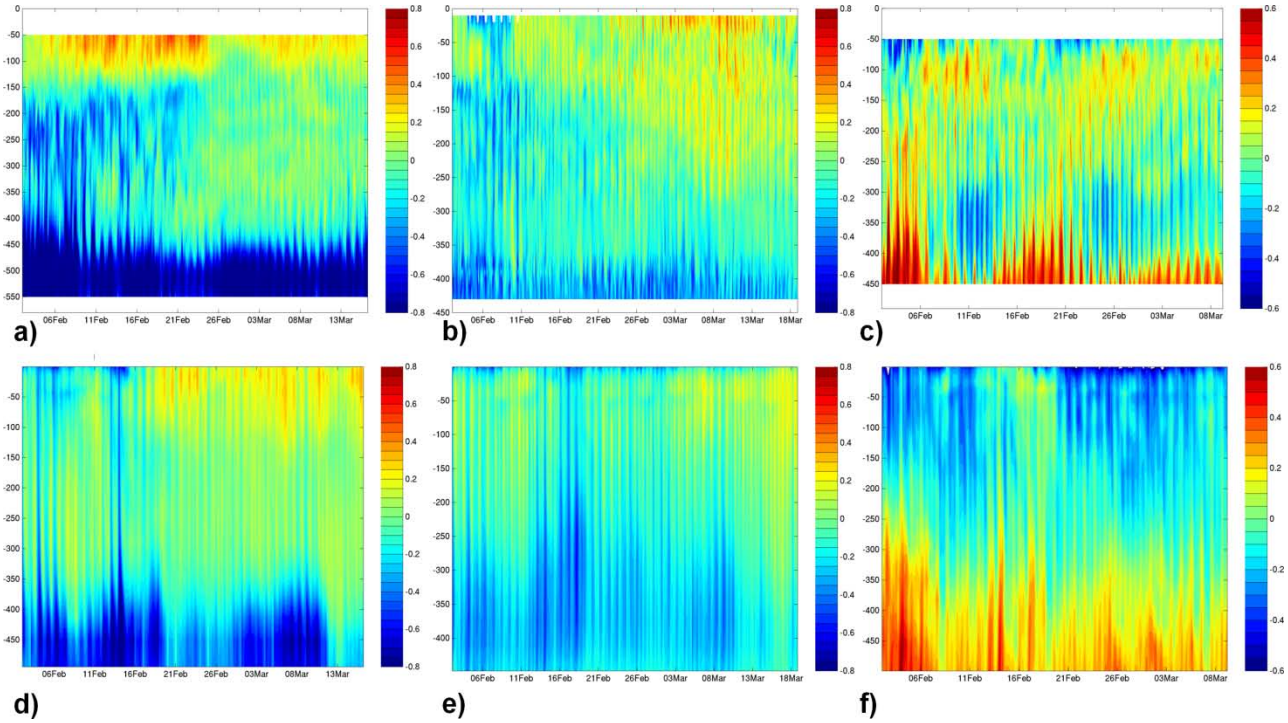

Figure 6 – Comparison of observed and modeled along-strait velocity over the period 2 Feb. 2009 until the recovery of each individual mooring. The top row is observations at moorings – a) Panay, b) Mindoro, c) Dipolog. The bottom row is model re-analysis estimates – d) Panay, e) Mindoro, f) Dipolog. The model estimates are in generally good agreement with the features of the observed flows, e.g. the bottom intensified flows especially at Panay and Dipolog, that even though no synoptic *in situ* data is utilized in the re-analysis.

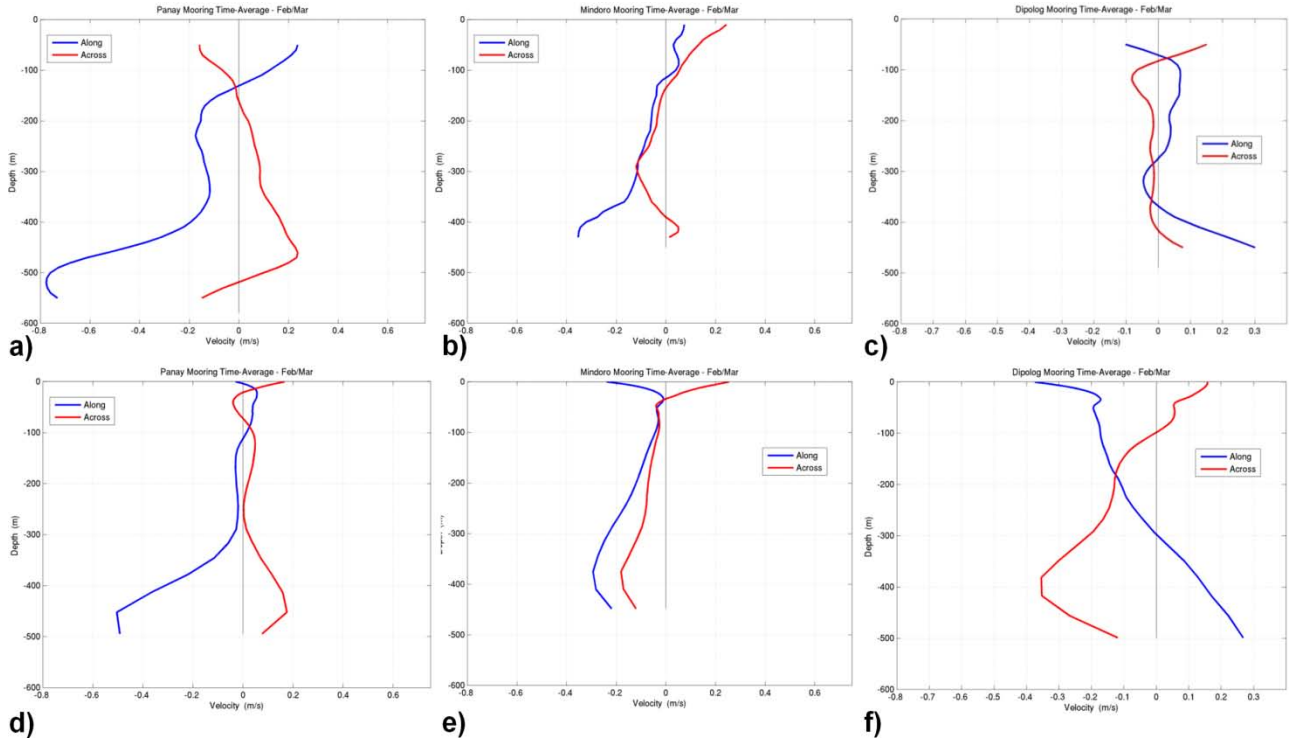

Figure 7 – Comparison of time-averaged along-strait (blue) and across-strait (red) velocities over the period 2 Feb. 2009 until the recovery of each individual mooring. The top row is observations at moorings – a) Panay, b) Mindoro, c) Dipolog. The bottom row is model re-analysis estimates – d) Panay, e) Mindoro, f) Dipolog. Even though no *in situ* data is assimilated, the structures of the simulated mean profiles overall agree with that of the observed means.

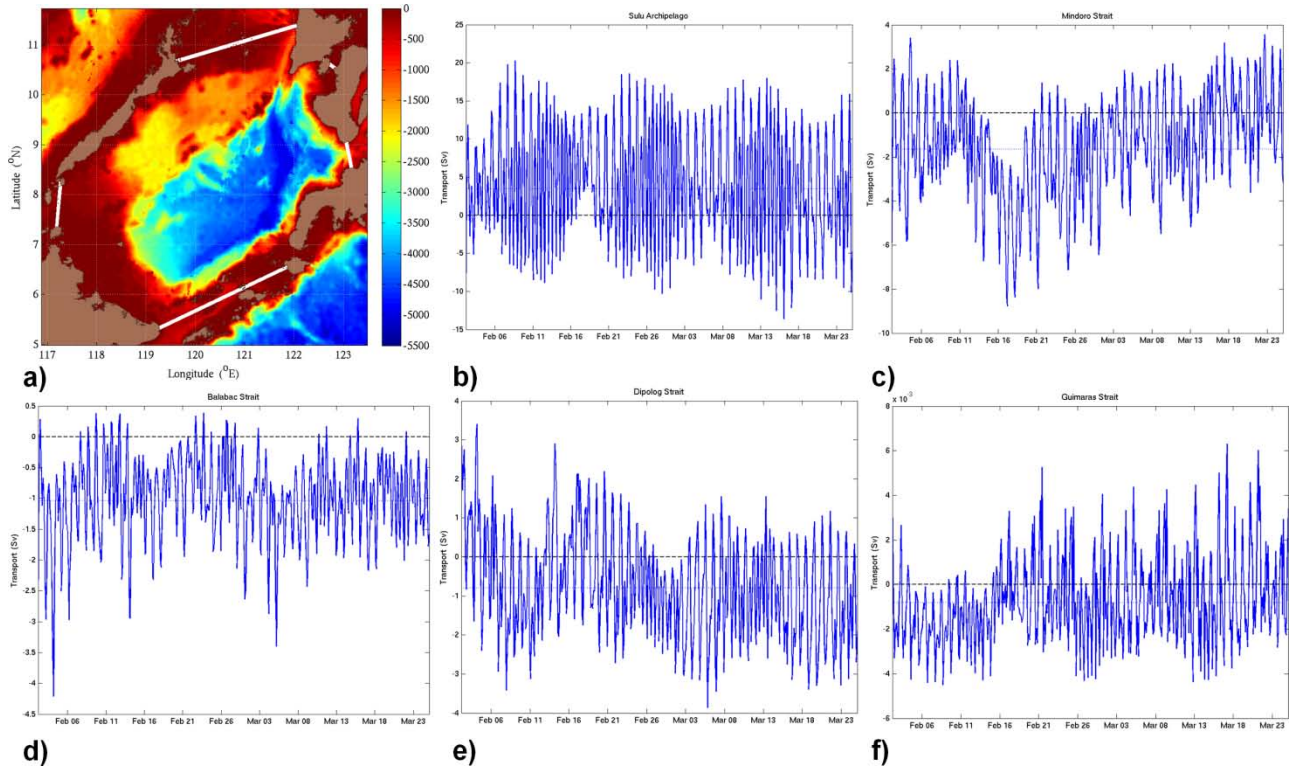

Figure 8 – Transports into and out of the Sulu sea (positive transports are out of the Sulu sea, for an outward normal) during Feb.-Mar. 2009. (a) Locations of the sections through which transports are evaluated, then transports as a function of time through the: (b) Sulu archipelago (+3.47 Sv time-average); (c) Mindoro strait (-1.65 Sv time-average); (d) Balabac strait (-1.04 Sv time-average); (e) Dipolog strait (-0.79 Sv time-average); and (f) Guimaras Strait(-8×10^{-4} Sv time-average).

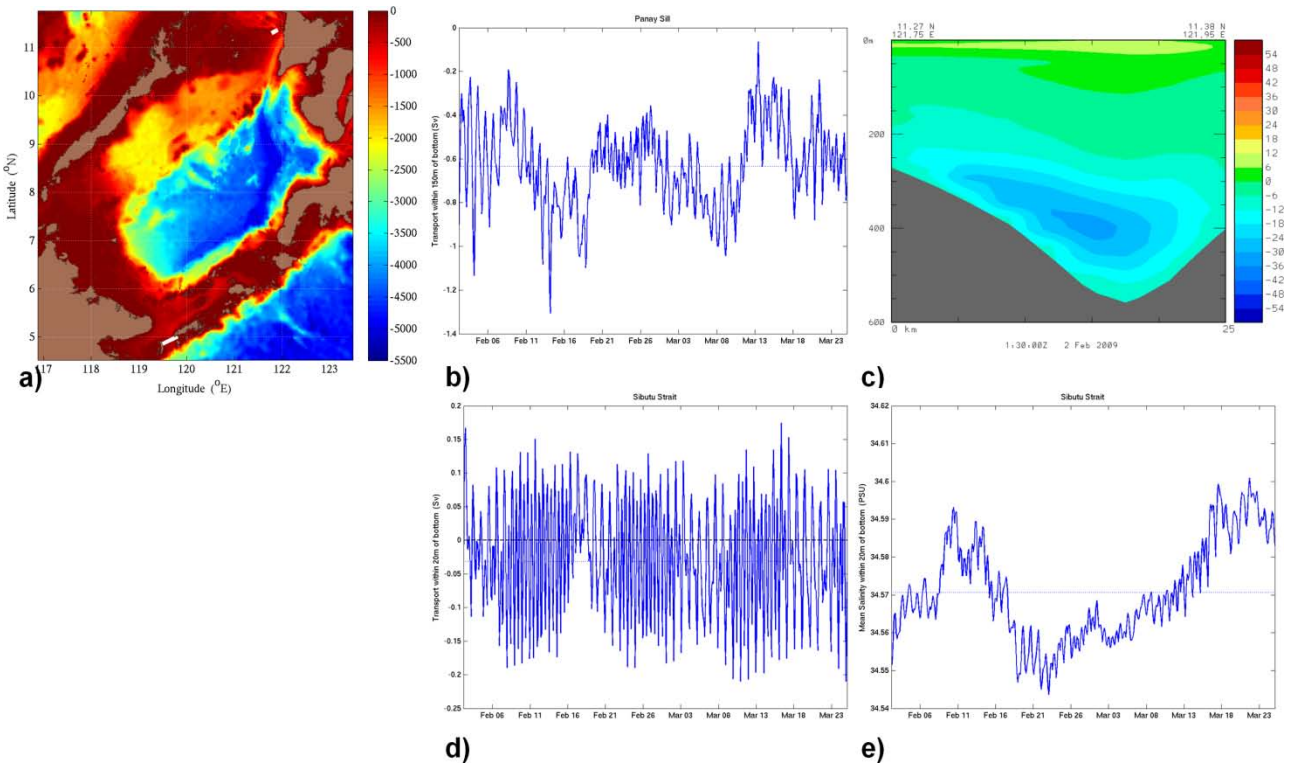

Figure 9 – Bottom water transports (Sv) over the Panay Sill and through the Sibutu Strait during Feb.-Mar. 2009. Positive transports are out of the Sulu Sea (outward normal). (a) Locations of sections for the Panay Sill proper and Sibutu Strait; (b) Transport versus time, over the Panay Sill within 150m of the bottom, providing a net time-average inflow of 0.645 Sv into the Sulu, with a 50% uncertainty standard deviation; (c) Velocity (cm/s, positive into the page), averaged over time during February-March 2009, over the Panay Sill, showing the westward deflection of the southern density-driven flow by the Coriolis force; (d) Transport versus time in the Sibutu Strait within 20m of the bottom, showing a small net time-average inflow of 0.032 Sv into the Sulu Sea; and (e) Mean salinity versus time in the Sibutu Strait within 20m of the bottom.

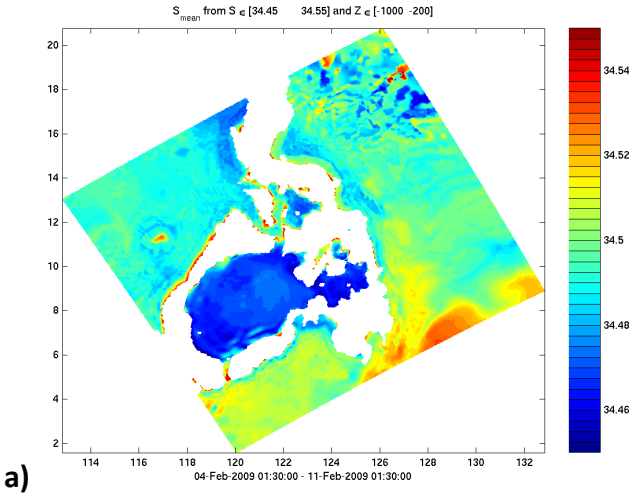
S mean from S ∈ [34.45 34.55] and Z ∈ [-1000 -200]
04-Feb-2009 01:30:00 - 11-Feb-2009 01:30:00

a)

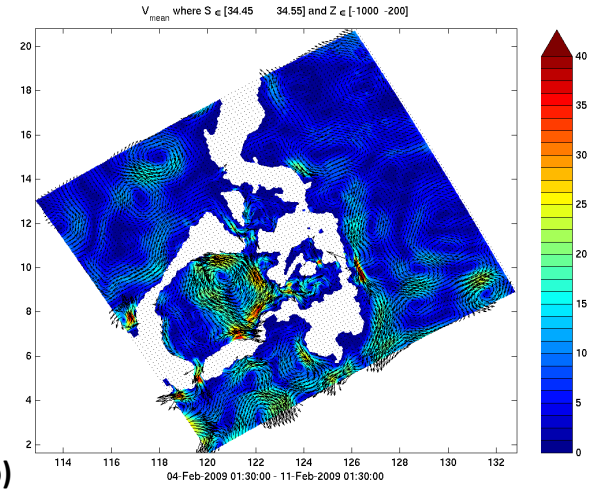
V mean where S ∈ [34.45 34.55] and Z ∈ [-1000 -200]
04-Feb-2009 01:30:00 - 11-Feb-2009 01:30:00

b)

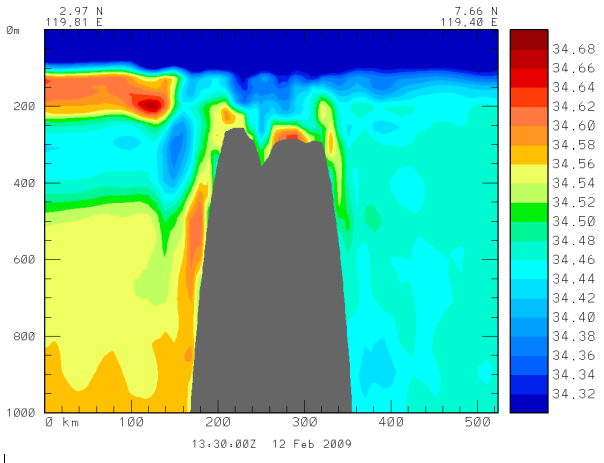
2.97 N
119.81 E
7.66 N
119.40 E
13:30:00Z 12 Feb 2009

c)

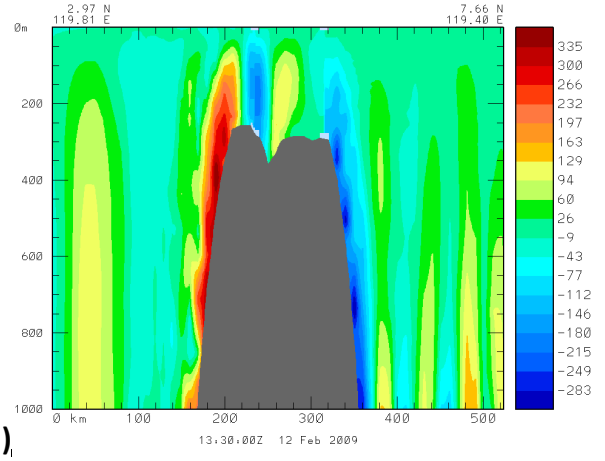
2.97 N
119.81 E
7.66 N
119.40 E
13:30:00Z 12 Feb 2009

d)

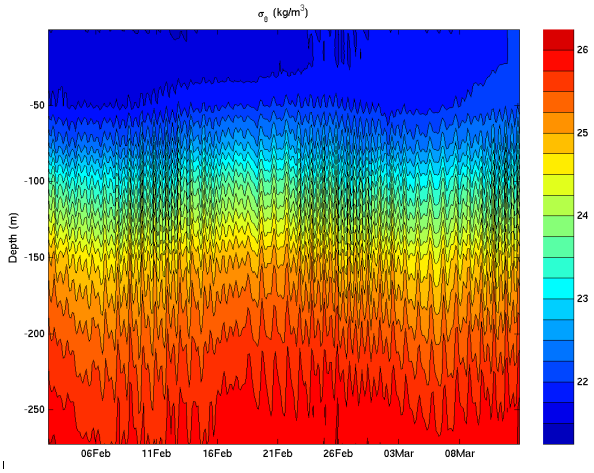
σθ (kg/m3)
Depth (m)

e)

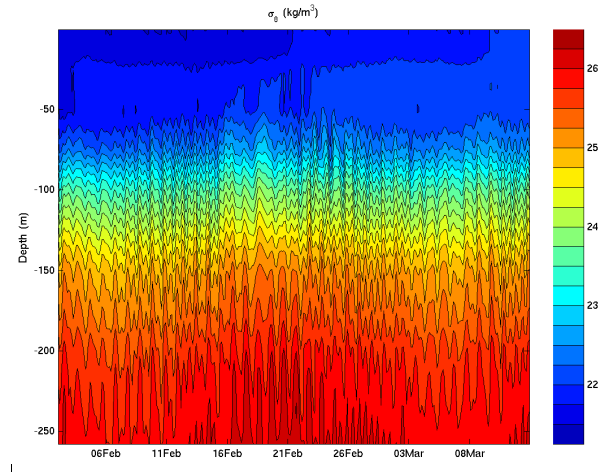
σθ (kg/m3)
Depth (m)

f)

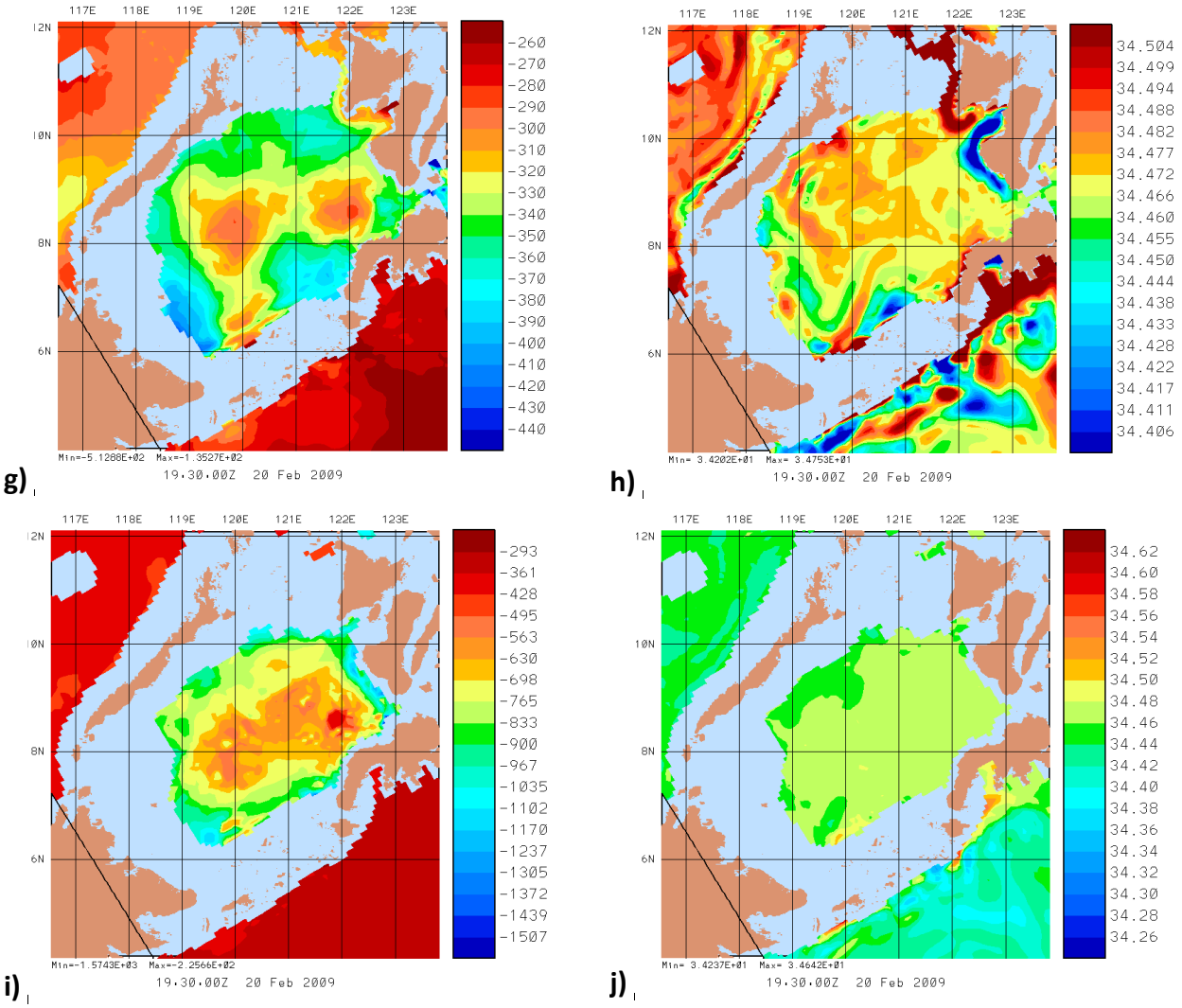

Figure 10. (a): Simulated salinity vertically-averaged from 200m to 1000m depths, but only if the salinity is within 34.45 to 34.55 (salinities outside that range are not considered), and temporally averaged over Feb. 4 to 11, 2009. (b): Corresponding vertically-integrated and temporally averaged horizontal velocity (cm/s). (c) and (d): Salinity and vertical velocity (m/day) snapshots, in a section along the Sibutu Strait from the Sulawesi to the Sulu, as estimated on 13:30Z, Feb. 12, 2009. (e) and (f): Potential density anomalies σ_θ as a function of time during Feb. 2 to Mar. 13, 2009, at the northern edge of Sibutu (5.8^{o}N, 119.5^{o}E) and at the steep northern shelfbreak of the Sulu Archipelago (6.2^{o}N, 120.3^{o}E), respectively. (g) and (h): Depth of the surface of constant potential density anomaly σ_θ=26.15 and the salinity on this surface, respectively, both estimated for 19:30Z on Feb 20, 2009. (i) and (j): as (g) and (h), but for the density anomaly σ_θ=26.50.